Progress In Electromagnetics Research M, Vol. 19, 25–38, 2011

TIME-DELAY-BASED MULTI-TARGET DETECTION AND POWER DELIVERING

X.-M. Zhong*, C. Liao, and W.-B. Lin

Institute of Electromagnetics, Southwest Jiaotong University, Chengdu 610031, China

Abstract—The paper presents an approach to locate and concentrate electromagnetic energy on targets based on time delays. An array of antennas is used in the approach, in which one antenna sends ultra-wide-band signals, and all antennas receive the signals backscattered by the targets. The time delays can be obtained by the interrelation of the transmitted and received signals. By controlling the timing of the pulses radiated from the individual antennas, high concentration of electromagnetic energy on the targets' locations can be achieved. The performance of this approach is demonstrated by several numerical simulations.

1. INTRODUCTION

Detecting unwelcome targets and providing high concentration of electromagnetic energy to destroy them has many applications in civil or military fields, such as hyperthermia treatment of cancer and other maladies, location and destruction of invading targets etc. Schwartz and Steinberg [1] demonstrate that the thinned transient arrays can achieve high concentration of electromagnetic energy and low side radiation with a very few elements. Baum [2] realizes it in focused aperture antennas. Hackett et al. [3] illustrate that the precise control of the pulses radiated from the individual transient elements allows the concentration of energy within regions where the pulses may overlap in a coherent fashion. Funk and Lee [4] show that precisely controlling the timing of pulses radiated from an array of N ultra-wide–band antennas produces a peak power that scales approximately as N^2 in directions where the pulses radiated from the individual elements combine coherently. These papers address the maximization of the

Received 25 April 2011, Accepted 10 June 2011, Scheduled 24 June 2011

* Corresponding author: Xuan-Ming Zhong (xm_zhong@163.com).

transient radiated field at a given far-field location, and only consider one-target case.

In this paper, an approach is presented for locating multiple targets and producing high concentration of electromagnetic energy on them. The technique utilizes an array of ultra-wideband antennas radiating short duration pulses to form a transient array, which is used to obtain the time delays for each target. At the same time, some constraint conditions are used to exclude the time delays that produced by physically nonexistent targets. Then the array can deliver high concentration of energy to the targets' locations based on the time delays. The validity of this approach is demonstrated with several numerical examples.

2. TIME DELAY ESTIMATION

In this paper, the pulse used in the antenna array is Gaussian, which can be written as

$$s(t) = \begin{cases} \exp\left[-10(2F_b\, t - 1)^2\right] & t \le 1/F_b \\ 0 & t > 1/F_b \end{cases} \tag{1}$$

where F_b can be defined as the maximum frequency of the pulse, and $T_b = 1/F_b$ is the pulse width. Suppose that there are M_t targets and that the array has N antennas. The array antennas are randomly set at the left of the simulation region, and the coordinate of the n-th antenna is denoted as $(x_{n-1},\ y_{n-1})$. Any one of the antenna can be selected as a proberwhich transmits the Gaussian pulse. All antennas will receive the signals backscattered by the M_t targets. The signal received by each antenna can be described as

$$r(t) = \sum_{i=1}^{M_p} \lambda_i s(t - \tau_i) + \omega(t) \quad 0 \le t \le T_r \tag{2}$$

where M_p is the number of multipath components. If the multiple scattering effects as well as mutual coupling between antennas can be ignored, M_p will be equal to M_t. $s(t)$ is the transmitted signal with duration T_s, and $\lambda_i,\ i = 1, 2, \ldots, M_p$ are the random multipath amplitudes taking into account of the target scattering characteristics and the propagation loss. τ_i is the time delay related to both scattering objects and paths. $\omega(t)$ is the additive white Gaussian noise (AWGN), and T_r is the duration of $r(t)$, i.e., the observation time. The sampled received signals can be written as

$$r(mT_{sp}) = \sum_{i=1}^{M_p} \lambda_i s(mT_{sp} - \tau_i) + \omega(mT_{sp}) \quad m = 0, 1, \ldots, K_r - 1 \tag{3}$$

where T_{sp} is the sampling period, and K_r is the number of samples. For convenience T_{sp} is normalized as $T_{sp} = 1$, and the n-th sample of $s(t-\tau_i)$ can be written as $s(n-\tau_i)$.

The time delay estimation can be done by matched filtering or cross-correlation [5]. Let $s(n)$ and $r(n)$ be zero-padded to length $K_A = K_r + K_s - 1$ where K_s is the length of $s(n)$. The cross-correlation function between $s(n)$ and $r(n)$ can be calculated through a circular correlation [5] as

$$R_A(\tau) = \sum_{n=0}^{K_A-1} s(n-\tau) \cdot r^*(n) \tag{4}$$

where the notation * denotes complex conjugate. We can also represent $s(n-\tau_i)$ in the IDFT form

$$s(n-\tau) = \sum_{k=0}^{K_A-1} \left[S(k) e^{-j2\pi k\tau/K_A} \right] e^{j2\pi kn/K_A} \tag{5}$$

where $S(k)$ is the DFT of $s(n)$ Plugging Eq. (5) into Eq. (4), we have

$$\begin{aligned} R_A(\tau) &= \sum_{n=0}^{K_A-1} \sum_{k=0}^{K_A-1} \left[S(k) e^{-j2\pi k\tau/K_A} \right] r^*(n) e^{j2\pi kn/K_A} \\ &= \sum_{k=0}^{K_A-1} [S(k) \cdot \gamma(k)] e^{-j2\pi k\tau/K_A} \\ &= \sum_{k=0}^{K_A-1} \left[\sum_{i=1}^{M_p} \lambda_i^* |S(k)|^2 e^{j2\pi k\tau_i/K_A} + W_A(k) \right] \times e^{-j2\pi k\tau/K_A} \end{aligned} \tag{6}$$

where

$$\begin{aligned} \gamma(k) &= \sum_{n=0}^{K_A-1} r^*(n) e^{j2\pi kn/K_A} = \sum_{n=0}^{K_A-1} \left[\sum_{i=1}^{M_p} \lambda_i s(n-\tau_i) + \omega(n) \right]^* e^{j2\pi kn/K_A} \\ &= \sum_{n=0}^{K_A-1} \left\{ \left[\sum_{i=1}^{M_p} \lambda_i s(n-\tau_i) + \omega(n) \right] e^{-j2\pi kn/K_A} \right\}^* \\ &= \left[\sum_{i=1}^{M_p} \lambda_i S(k) e^{-j2\pi k\tau_i/K_A} + W(k) \right]^* \end{aligned}$$

and $W_A(k) = S(k) \cdot W^*(k) W(k)$ is the DFT of $\omega(t)$. The time delays can be estimated by the peaks of the envelope of $R_A(\tau)$ in (6). However,

they are unable to separate the true peaks which correspond to the different time delays but are spaced less than the resolution limit. From (6), $R_A(\tau)$ can be mathematically considered as the DFT of $x_A(k)$, where $x_A(k)$ is denoted as

$$x_A(k) = \sum_{i=1}^{M_p} \lambda_i^* \left|S(k)\right|^2 e^{j2\pi k\tau_i/K_A} + W_A(k) \tag{7}$$

Furthermore, the squared envelope of $R_A(\tau)$ can be viewed as the power spectrum of $x_A(k)$, and we have the following relation

$$\left|R_A(\tau)\right|^2 = \left|DFT\left[x_A(k)\right]\right|^2 \tag{8}$$

In vector form, the data model in (7) can be represented by

$$\mathbf{x}_A = \sum_{i=1}^{M_p} \lambda_i^* \Lambda(\tau_i) S + \mathbf{W}_A \tag{9}$$

where

$$\begin{aligned}
\mathbf{x}_A &= \left[x_A(0)\ x_A(1)\ \ldots\ x_A(K_A-1)\right]^T \\
\lambda_A &= \left[\lambda_1^*\ \lambda_2^*\ \ldots\ \lambda_{M_p}^*\right]^T \\
\mathbf{\Lambda}(\tau_i) &= \mathrm{diag}\left(1 e^{j2\pi\tau_i/K_A} \ldots e^{j2\pi\tau_i(K_A-1)/K_A}\right) \\
S &= \left[\left|S(0)\right|^2\ \left|S(1)\right|^2\ \ldots\ \left|S(K_A-1)\right|^2\right] \\
\mathbf{W}_A &= \left[W_A(0)\ W_A(1)\ \ldots\ W_A(K_A-1)\right]^T
\end{aligned}$$

Based on the Wiener-Khinchine theorem [5], the correlation function of x_A can be written as

$$Rx_A(l) = DFT^{-1}[\left|\bar{R}_A(\tau)\right|^2], \quad l = 0, 1, \ldots, 2K_A - 1 \tag{10}$$

where $\left|\bar{R}_A(\tau)\right|^2$ is a sequence formed by zero-padding $\left|R_A(\tau)\right|^2$ to length $2K_A - 1$. Therefore, the estimated covariance matrix $\mathbf{R}x_A$ can be formed based on the elements of the sequence $Rx_A(l)$ as [6]

$$\mathbf{R}x_A = [R_{Aij}]_{M_A \times M_A} \tag{11}$$

where $R_{Aij} = Rx_A(i-j)$ for $i \geq j$, and $R_{Aij} = R_{Aij}^*$ for $i < j$, $M_A = \lfloor (K_A+1)/2 \rfloor$, and $\lfloor \chi \rfloor$ denotes the largest integer no greater than χ. According to [6], $\mathbf{R}x_A$ is full rank. In the eigen-decomposition of $\mathbf{R}x_A$, the dimensions with eigenvalues close to zero belong to the noise subspace G_A. The dimensions with larger eigenvalues are identified as the signal subspace. Similar to the derivation of MUSIC [7], the signal subspace should be orthogonal to the noise subspace. The time delay

τ_i with $i = 1, 2, \ldots, M_p$ can be obtained by locating the M_p maxima of

$$P_A(\tau) = \frac{1}{S^H \Lambda_A^H(\tau) G_A G_A^H \Lambda_A(\tau) S} \tag{12}$$

where S is an $M_A \times 1$ sub-vector formed by $|S(k)|^2$, and $\mathbf{\Lambda}_A(\tau_i) = \text{diag}\left(1 e^{j2\pi\tau/K_A} \ldots e^{j2\pi\tau(M_A-1)/K_A}\right)$.

The algorithm to obtain the time delay estimation for all antennas can be summarized as follows:

Step 1. Compute the cross-correlation function between $s(n)$ and $r(n)$ in Eq. (3) to obtain as $R_A(\tau)$ in Eq. (4).

Step 2. Zero-pad $|R_A(\tau)|^2$ to get $\left|\bar{R}_A(\tau)\right|^2$, and compute IDFT of $\left|\bar{R}_A(\tau)\right|^2$ as in Eq. (10), then form the estimate $\mathbf{R}x_A$ as in Eq. (11).

Step 3. Eigendecompose $\mathbf{R}x_A$ to obtain G_A, and estimate τ_i, $i = 1, 2, \ldots, N$, basing on Eq. (12).

In the last step, N time delays are obtained corresponding to each antenna, since the number of antennas is known, and N is always set larger than M_t [8, 9].

3. CONSTRAINT CONDITION

It is assumed that the array considered here is made up of N antennas, and there are totally M_t targets. When an antenna transmits electromagnetic wave, all antennas will receive a set of data which are from M_p paths and backscattered by the M_t targets. Based on the data from the n-th antenna, we can obtain the time delay estimation τ_{ni}, $n = 1, 2, \ldots, N$, $i = 1, 2, \ldots, M_p$ with the transmitted pulse as reference signal.

However, we can not take it for granted that the time delay τ_{ni}, $n = 1, 2, \ldots, N$, is directly produced by the i-th target, since it is possible that the i-th time delay in the n-th element directly or indirectly corresponds to any one of the targets. Any combination of one time delay randomly picked from each antenna forms a set of time delays, which includes the sets of time delays directly produced by real targets if the separation between targets is large enough. The next work needs to be determined if it is directly due to the same real scattering target or physically nonexistent targets that must be removed.

It is well known that the locus of points for a constant difference in time arrival of pulses from the two stationary omnidirectional point sources forms a hyperboloid of revolution where the sources are located at the foci of the hyperboloid [3]. Consequently, for a given time delay between the two pulses radiated from fixed wideband omnidirectional

sources in a plane, a coherent overlap of the radiated pulses will occur at the points that fall on a hyperbola as shown in Fig. 2. Note that for a specific time delay between the two radiated pulses, the coherent overlap occurs at the points along only one leg of the hyperbola.

Now lets consider the case that there are N sources shown in Fig. 2. Suppose τ_{ni}, $n = 1, 2, \ldots, N$, is a set of time delays from the ith target. First we should consider only two sources at a time in looking for the coherence. The total number of hyperbolas will be the sum of the combination number of sources taken two at a time. However, only $N-1$ hyperbolas are independent for the N sources. There will be a total of $C_N^2 = (N-1)N/2$ hyperbolas with only $N-1$ hyperbolas needed to establish the common coherency point, where the $(N-1)N/2$ hyperbolas have a common intersection point.

For example, we take the antenna at (x_0, y_0) as a reference antenna. The antenna at (x_0, y_0) and any one of other antennas in the array will located at the focus of one hyperboloid. The general equation for the hyperbola can be written as

$$\sqrt{(x-x_0)^2 + (y-y_0)^2} - \sqrt{(x-x_n)^2 + (y-y_n)^2} = c\tau_n \qquad (13)$$

Here c is propagation speed in the ambient medium, and $\tau_n = \tau_{ni} - \tau_{0i}$ is the propagation time delay difference from the antennas at (x_0, y_0) and (x_n, y_n) which are located at the foci of the hyperbola. There are $N-1$ hyperboloids for the reference antenna at (x_0, y_0). If $\tau_n > 0$, the pulse radiated from the n-th source must be delayed by τ_n, and the propagation path from the n-th source is less than the path from the first source, and vice versa. For the target 1 shown in Fig. 1, the time delay estimation τ_{n1}, $n = 1, 2, \ldots, N-1$, is physical. The target

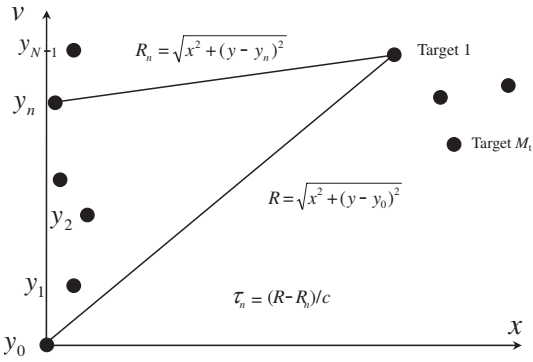

Figure 1. An illustration of a line of N antennas placed along the y axis.

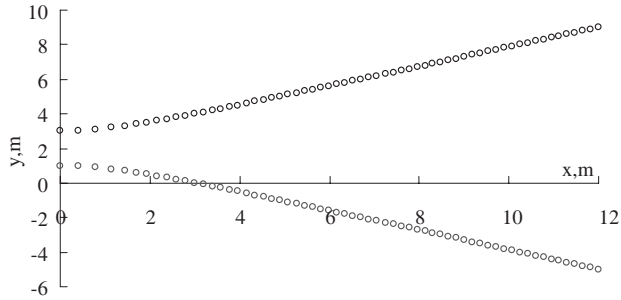

Figure 2. A hyperbola with foci at (0, 0) and (4, 0).

locates at the intersection of the $N-1$ hyperboloids. Otherwise, if the target does not locate at the intersection of all hyperboloids, the set of time delays is nonphysical and should be removed. Suppose the two antennas are located at $(0,0)$and $(0,4)$, and the time delay $\tau_n = 6.667\,\text{nS}$, we have the hyperbola as shown in Fig. 2. It is worth noting that the constraint condition (13) is only valid for the homogeneous medium, but is independent to source types. Therefore, this algorithm can work for the homogeneous environments with other sources such as acoustic, but not for the inhomogeneous environments.

4. RADIATED POWER

For the analysis of pulse radiation from a linear array, some simplifications are made. It is assumed that the separation between arrays is large enough and the mutual coupling between antennas can be ignored. The radiated electric field in the far region from the n-th antenna in the array may be written as:

$$\vec{E}_n = \vec{E}_0 F(\theta,\varphi) e^{j\xi_n} e^{-jkL_n}/L_n \tag{14}$$

where E_0 is the radiated maximum electric field, $F(\theta,\varphi)$ is the direction function of each antenna, ξ_n is initial phase, k is the propagation constant in the ambient medium, L_n is the distance from the n-th element to the target. Based on the principle of superposition, the total maximum electric field at the target location from N sources is simply the vector addition of the field vectors produced by each source.

$$\vec{E} = \sum_{n=1}^{N} \vec{E}_n = \sum_{n=1}^{N} \vec{E}_0 e^{j\xi_n} e^{-jkL_n}/L_n \tag{15}$$

In the far region, $1/L_1 \approx 1/L_2 \approx \ldots \approx 1/L_N = 1/L$, and Eq. (15) can be simplified as

$$\vec{E} = \frac{\vec{E}_0}{L} \sum_{n=1}^{N} e^{j\xi_n} e^{-jkL_n} \tag{16}$$

The total radiated power at the target location can be written as

$$P \propto \left|\vec{E}\right|^2 = \left(\frac{E_0}{L}N\right)^2 \frac{N + \sum\limits_{n=1,m=1}^{N} \sum\limits_{n\neq m}^{N} \cos(\Delta\theta_{nm})}{N^2} \tag{17}$$

where $\Delta\theta_{nm} = \theta_n - \theta_m,\ n = 1, 2, \ldots, N,\ m = 1, 2, \ldots, N,\ n \neq m$, is the phase difference between the signals from the n-th antenna and the one from the m-th antenna $\theta_n = \xi_n - kL_n n = 1, 2, \ldots, N$, is the phase of the signal at the target location from the n-th antenna. Theoretically, it can be drawn from Eq. (17) that the total radiated power will have the maximum value of $(E_0 N/L)^2$ if $\cos(\Delta\theta_{ni}) = 1$, which is N^2 times that of a single antenna.

5. NUMERICAL RESULTS AND ANALYSIS

In order to demonstrate the performance of this method, we take 2D electromagnetic simulations as examples. We employ Finite-difference-time-domain (FDTD) method to do the simulations. An array which consists of 4 antennas elements is considered. The antennas are located along the y axis as: $x_0 = 0\,\text{m}$, $y_0 = 0.98\,\text{m}$, $x_1 = 0\,\text{m}$, $y_1 = 1.76\,\text{m}$, $x_2 = 0\,\text{m}$, $y_2 = 2.54\,\text{m}$, $x_3 = 0\,\text{m}$, $y_3 = 3.32\,\text{m}$. Two targets are respectively located at (3.09 m, 1.89 m) and (3.62 m, 2.42 m). The 4th antenna is selected to emit the Gaussian pulse, whose width is $T_b = 0.33\,\text{nS}$. Each antenna will receive a set of data backscattered by the two targets. Based on Eq. (12), we have the time delays received at the 4 antennas as follows:

$$\begin{aligned}
&\text{The 1st antenna: } 22.78\ 23.09\ 24.97\ 25.31\ \text{nS}\\
&\text{The 2nd antenna: } 21.96\ 22.27\ 24.61\ 24.96\ \text{nS}\\
&\text{The 3rd antenna: } 21.74\ 22.06\ 24.80\ 25.15\ \text{nS}\\
&\text{The 4th antenna: } 22.16\ 22.47\ 25.52\ 25.85\ \text{nS}
\end{aligned} \tag{18}$$

Since there exists multiple scattering between the targets, there are more than two time delays received at each antenna as shown in (18). Constraint condition (13) is used to remove the non-physical time delays due to the multiple scattering. If the distance of all hyperboloids' intersections produced by Eq. (13) is smaller than the wave length which corresponds to the maximum frequency of the

pulse, this set of time delays is taken as the real set of time delays directly produced by a target. Otherwise, it is removed by the method and taken as a set of time delays from a non-physical target. Here $\lambda = cT_b = 0.1$ m. Therefore, only two sets of time delays are left.

$$\begin{aligned} &\text{The 1st antenna: } 22.78\ 24.97 \text{ nS} \\ &\text{The 2nd antenna: } 21.96\ 24.61 \text{ nS} \\ &\text{The 3rd antenna: } 21.74\ 24.80 \text{ nS} \\ &\text{The 4th antenna: } 22.16\ 25.52 \text{ nS} \end{aligned} \tag{19}$$

The relative time delay is respectively (22.78, 21.96, 21.74, 22.16) nS and (24.97, 24.61, 24.80, 24.52) nS. Based on the data of the time delays for each antenna, we can make the following arrangements: The Gaussian pulse is radiated from the 1st and 2nd antennas after 22.78 nS and 2196 nS, and the 3rd and 4th antennas radiate the identical pulse after 21.74 nS and 2216 nS, respectively. With these parameters, a set of three hyperbolas are obtained to illustrate the coherence points as shown in Fig. 3. As expected, the three hyperbolas intersect at the first target location (3.09 m, 1.89 m). Fig. 4 shows the electromagnetic energy distribution radiated from these four antennas with the above parameters. It can be seen clearly that the energy is concentrated at the location of (3.09 m, 1.89 m). The ratio of the combined energy peak at the target location to the radiated energy peak by the individual antenna is 0.9621%.

In contrast, Fig. 5 shows the energy distribution for the case with no time delay, in which the Gaussian pulses are radiated by the four antennas at the same time. In this case, the ratio of the combined energy peak at the target location to the radiated energy peak by the individual antenna is only 0.1173%.

Note that the ratio of the energy peak at target location to the radiated energy peak for one individual antenna is about 0.0607% and

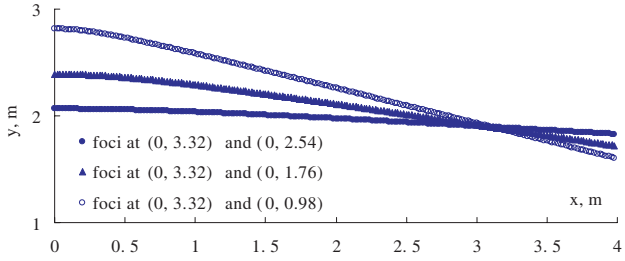

Figure 3. The hyperbolas obtained from four sources located along the y axis with a target located at (3.09 m, 1.89 m).

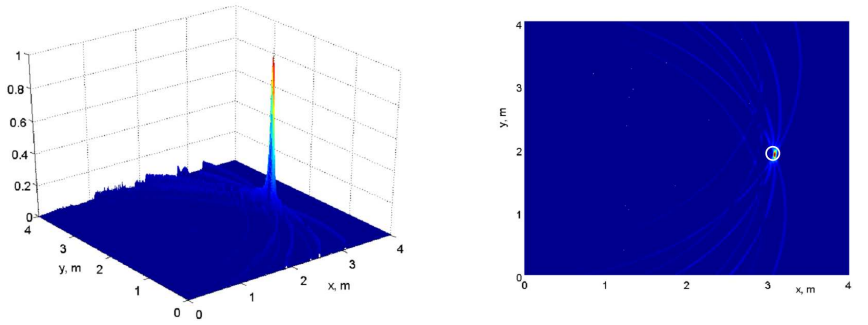

(a) 3-D map of energy distribution (b) 2-D map of energy distribution

Figure 4. The energy distribution map for a four-antenna array with the 1st set of relative time delays (22.78, 21.96, 21.74, 22.16) nS.

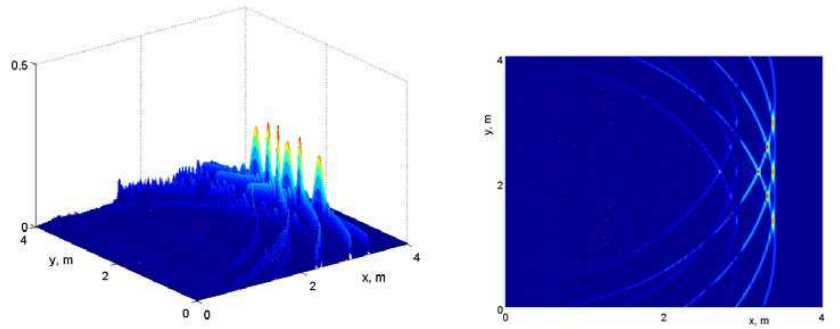

(a) 3-D map of energy distribution (b) 2-D map of energy distribution

Figure 5. The energy distribution for a four-antenna array with no time delays.

that the theoretical results predicted by Eq. (17) is $4^2 \times 0.0607\% = 0.9707\%$. The numerical simulation result in Fig. 4 is 0.9621%, which is very close to theoretical results.

If the Gaussian pulse is radiated from the 1st and 2nd antennas after 24.97 nS and 24.61 nS, and the 3rd and 4th antennas radiate the identical pulse after 2480 nS and 24.52 nS, respectively. The energy will concentrate at the location of the second target (3.62 m, 2.42 m) as shown in Fig. 6, and the ratio of the combined energy peak at the target location to the radiated energy peak by the individual antenna is 0.8129%, in contrast to 0.0991% in the case with no time delay.

In order to show the effectiveness of this method, another

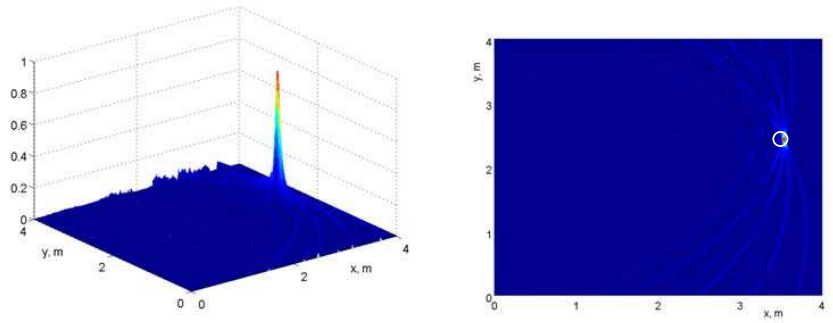

(a) 3-D map of energy distribution (b) 2-D map of energy distribution

Figure 6. The energy distribution map for a four-antenna array with the 2nd set of relative time delays (24.97, 24.61, 24.80, 24.52) nS.

numerical simulation is given. An array which consists of 9 antennas is considered. The positions of antennas are randomly chosen at the left of the simulation region as: (0, 0.21 m), (0.1 m, 0.69 m), (0.2 m, 1.18 m), (0.1 m, 1.67 m), (0.3 m, 2.16 m), (0.1 m, 2.64 m), (0.2 m, 3.13 m), (0.1, 3.62), (0, 4.11 m). Four targets are respectively located at (2.36 m, 1.49 m), (3.03 m, 1.83 m), (3.03 m, 2.49 m) and (3.69 m, 2.83 m). The 4th target at (3.69 m, 2.83 m) is the weakest reflective one whose reflection factor is only half of the other targets. The 5th antenna is selected to emit the Gaussian pulse. Each antenna will receive a set of data backscattered by the four targets. Based on Eq. (12), we have the time delays received at the 9 antennas with respect to the transmitted pulse as follows:

antenna 1: 16.22 16.99 20.65 20.88 21.22 21.85 22.40 26.72 27.14 nS
antenna 2: 15.25 15.54 19.67 19.91 20.24 20.67 21.22 25.52 25.84 nS
antenna 3: 14.54 14.83 15.07 18.88 19.62 19.91 20.16 20.47 24.46 nS
antenna 4: 14.82 15.36 18.98 19.36 19.93 24.17 24.79 25.41 25.03 nS
antenna 5: 14.48 14.76 14.99 18.37 18.96 19.28 23.13 23.61 24.89 nS
antenna 6: 15.71 15.99 16.23 18.35 19.07 20.17 21.62 23.58 24.22 nS
antenna 7: 16.30 17.49 18.88 19.35 19.61 20.15 20.96 23.28 23.85 nS
antenna 8: 17.60 17.87 18.18 19.67 20.14 20.66 21.20 23.85 24.48 nS
antenna 9: 19.00 19.28 20.65 20.88 21.84 22.39 22.76 24.62 25.57 nS (20)

The constraint condition (13) is used to remove the non-physical time delays due to the multiple scattering Therefore, only four sets of

time delays are left.

$$\begin{aligned}
&\text{target 1: } 16.22\ 15.25\ 14.54\ 14.82\ 14.48\ 15.71\ 16.30\ 17.60\ 19.00\,\text{nS}\\
&\text{target 2: } 20.65\ 19.67\ 18.88\ 18.98\ 18.37\ 18.35\ 19.61\ 20.66\ 21.84\,\text{nS}\\
&\text{target 3: } 21.85\ 20.67\ 19.62\ 19.36\ 18.37\ 19.07\ 18.88\ 19.67\ 20.65\,\text{nS}\\
&\text{target 4: } 26.72\ 25.52\ 24.46\ 24.17\ 23.13\ 23.58\ 23.28\ 23.85\ 24.62\,\text{nS}
\end{aligned} \tag{21}$$

If the Gaussian pulse is radiated from each array antenna based on the time delays in (21), the energy will concentrate at the locations of the targets. Fig. 7 shows the energy concentration on the 4th target. The ratio of the combined energy peak at the target location to the radiated energy peak by the individual antenna is 1.908%, in contrast to 0.044% in the case with no time delay at the target location.

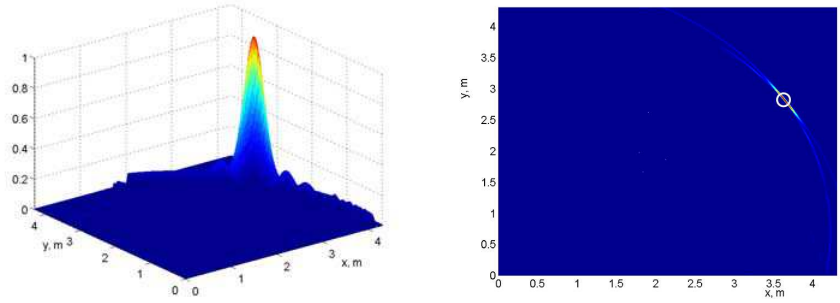

(a) 3-D map of energy distribution (b) 2-D map of energy distribution

Figure 7. The energy distribution map for a nine-antenna array with the set of relative time delays (26.72, 25.52, 24.46, 24.17, 23.13, 23.58, 23.28, 23.85, 24.62) nS.

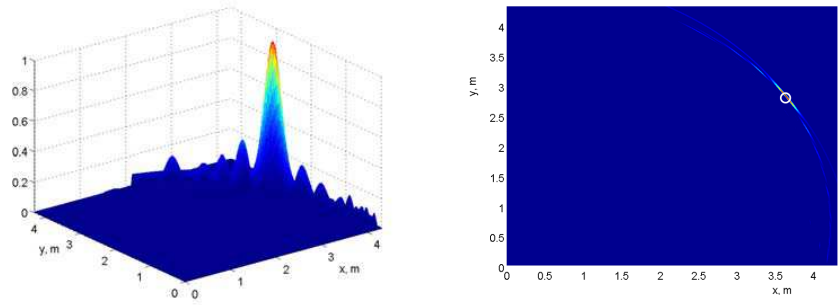

(a) 3-D map of energy distribution (b) 2-D map of energy distribution

Figure 8. The energy distribution map for the DORT method with a nine-antenna array.

In order to show the performance of this method, the decomposition of reverse time operator (DORT) method in [8–14] is employed as a reference. Fig. 8 shows the energy concentration on the 4th target. Although the 2-D maps of energy distribution look almost same, the ratio of the combined energy peak at the target location to the radiated energy peak by the individual antenna for the DORT is 1.847%, in contrast to 1.908% in our method.

6. CONCLUSION

A novel approach with the time delays to locate and concentrate electromagnetic energy on targets is presented. One antenna in the array emits an UWB pulse, and all antennas receive the signals backscattered by the targets. The time delays can be obtained based on the mutual relation of the transmitted signal and the received ones. Since the multiple scatterings among targets exist, the number of time delay sets for each antenna is more than the number of the targets. Therefore, the constraint condition is studied to remove the nonphysical time delay sets. Based on the obtained time delay, the energy radiated by each antenna will concentrate on the targets location where the pulses from the individual antennas combine coherently. The validity of this approach is finally demonstrated with numerical electromagnetic simulations.

ACKNOWLEDGMENT

This work was supported by the NSAF of China (Grant No. 11076022) and the Fundamental Research Funds for the Central Universities, project # SWJTU09ZT39 and the Opening Project of Key Laboratory of Cognitive Radio and Information Processing (Guilin University of Electronic Technology), Ministry of Education.

REFERENCES

1. Schwartz, J. L. and B. D. Steinberg, "Properties of ultrawideband arrays," *Ultra-wideband, Short-pulse Electromagnetics 3*, C. E. Baum, Ed., 139–145, Plenum, New York, 1997.
2. Baum, C. E., "Focused aperture antennas," Air Force Research Laboratory Sensor and Simulation Notes, No. 306, Kirtland AFB, NM, May 1987.
3. Hackett, R. D., C. D. Taylor, D. P. McLemore, H. Dogliani, W. A. Walton, III, and A. J. Leyendecker, "A transient array to

increase the peak power delivered to a localized region in space: Part I — Theory and modeling," *IEEE Trans. Antennas Propaga.*, Vol. 50, No. 12, 1743–1750, 2002.

4. Funk, E. E. and C. H. Lee, "Free-space power combining and beam steering of ultra-wideband radiation using an array of laser-triggered antennas," *IEEE Trans. Microwave Theory Tech.*, Vol. 44, 2039–2044, Nov. 1996.
5. Proakis, J. G. and D. G. Manolakis, *Digital Signal Processing: Principles, Algorithms, and Applications*, 3rd edition, Prentice Hall, Englewood Cliffs, NJ, 1996.
6. Ren, Q. S. and A. J. Willis, "Extending MUSIC to single snapshot and on line direction finding applications," *Proceedings of the Radar Edinburgh International Conference*, No. 449, 783–787, 1997.
7. Schmidt, R. O., "Multiple emitter location and signal parameter estimation," *IEEE Trans. Antennas Propag.*, Vol. 34, No. 3, 276–280, Mar. 1986.
8. Yavuz, M. E. and F. L. Teixeira, "Full time-domain DORT for ultrawideband electromagnetic fields in dispersive, random inhomogeneous media," *IEEE Trans. Antennas Propag.*, Vol. 54, No. 8, 2305–2315, Aug. 2006.
9. Micolau, G., M. Saillard, and P. Borderies, "DORT method as applied to ultrawideband signals for detection of buried objects," *IEEE Trans. Geosci. Remote Sensing*, Vol. 41, No. 8, 1813–1820, Aug. 2003.
10. Kosmas, P. and C. King's, "Application of the DORT technique to FDTD-based time reversal for microwave breast cancer detection," *European Microwave Conference*, 306–308, Oct. 2007.
11. Xiao, S.-Q., J. Chen, B.-Z. Wang, and X.-F. Liu, "A numerical study on time-reversal electromagnetic wave for indoor ultrawideband signal transmission," *Progress In Electromagnetics Research*, Vol. 63, 329–342, 2007.
12. Zhang, W., A. Hoorfar, and L. Li, "Through-the-wall target location with time reversal MUSIC method," *Progress In Electromagnetics Research*, Vol. 106, 75–89, 2010.
13. Lazaro, A., D. Girbau, and R. Villarino, "Wavelet-based breast tumor localization technique using an UWB radar," *Progress In Electromagnetics Research*, Vol. 98, 75–95, 2009.
14. Lazaro, A., D. Girbau, and R. Villarino, "Weighted centroid method for breast tumor localization using an UWB radar," *Progress In Electromagnetics Research B*, Vol. 24, 1–15, 2010.